LUBRICATION SCIENCE
Lubrication Science 2012; **24**:1–10
Published online 24 August 2011 in Wiley Online Library (wileyonlinelibrary.com). DOI: 10.1002/ls.163

Molecular dynamics simulation of intrusion of a C60 molecule ball into sliding contact space

Pei Li and Dongfeng Diao*,†

Key Laboratory of Education Ministry for Modern Design and Rotor-Bearing System, School of Mechanical Engineering, Xi'an Jiaotong University, Xi'an 710049, China

ABSTRACT

The intrusion process of a C60 ball into a sliding contact space with an included angle made up by two silicon substrates (100) was simulated using the molecular dynamics approach. The simulation was carried out using Tersoff potential of C and Si atoms at room temperature of 300 K. The included angle was defined as initial entry angle changing from 20° to 90° in the simulation for studying the effect of the initial entry angle during the intrusion process. The dependence of the initial entry angle on the number of sticking Si atoms of upper substrate was calculated. The results showed that the number of sticking atoms increased with the increasing of initial entry angle, and the number of sticking atoms was divided into three regions with different slopes, which could be used to evaluate the intrusion performance of a C60 ball into the sliding contact space. Copyright © 2011 John Wiley & Sons, Ltd.

Received 13 January 2011; Revised 28 April 2011; Accepted 7 June 2011

KEY WORDS: molecular dynamics simulation; sliding contact space; C60 ball; intrusion; number of stickling atoms; critical initial entry angle

INTRODUCTION

The cleaning system of particles is an important tribosystem in laser printers; the leftover particles attached to the surface of an organic photoconductor roller must be removed by the sliding of a blade against the roller.[1] At present, the development of printing technology is faced with the scientific problem on how to clean a spherical particle when its size is going to nanometre. To find a better way to clean the nano particles, the first question to be solved is how a particle intrudes into the sliding contact space. Thus, the study of the state of motion and the critical intrusion condition of the nano particle in a sliding contact space becomes important. In this study, we choose the C60 ball as a nano particle to simulate the intrusion process.

An arbitrary particle may slide, roll and rotate on a flat surface, and the experimental investigation on the motion of particle on surfaces was conducted with the aid of micromanipulators.[2–4]

*Correspondence to: Dongfeng Diao, Key Laboratory of Education Ministry for Modern Design and Rotor-Bearing System, School of Mechanical Engineering, Xi'an Jiaotong University, Xi'an 710049, China.
†E-mail: dfdiao@mail.xjtu.edu.cn

M.D. Murthy Peri *et al*. performed atomic force microscope experiments and showed that the rolling resistance moment exhibited by a spherical particle bonded to substrate is an important measure for studying interfacial forces and particle removal processes, as well as measuring the work of adhesion.[2,3] Metin Sitti and Hideki Hashimoto performed a pushing study on particles on a silicon substrate with an Atomic Force Microscopy probe and analysed the interaction forces between the microsphere, the substrate and the manipulation probe. The sliding, rolling and rotational motions of the particles were observed.[4] The size of the particle used in the experiments mentioned earlier was in micro scale. However, at nano scale, the surface forces and surface phenomena will become dominant, and thus, a deep insight into the particle-surface interaction is required. Molecular dynamics simulation is a powerful computational method for studying nanoscale surface phenomena, and thus, the atomic-scale interactions between a particle or a nano-cluster and a substrate were investigated using molecular dynamics simulation.[5–16] Liangchi Zhang and Hiroaki Tanaka reported the friction and wear mechanisms in silicon associated with a two-body or a three-body contact sliding.[11] W.G. Lee *et al*. studied the rolling resistance of a sphere on an atomically flat surface. Their work revealed that rolling friction at the nanoscale level was similar to the macroscopic rolling condition during strain hardening of metals.[12] D.S. Rimai *et al*. discussed the particle adhesion form micrometre-size scale to nanometre-size.[13] The contact area and adhesion energy as the particle impinging onto the substrate were investigated by Paolo Valentini and Traian Dumitrica.[14] The interaction of energetic fullerene molecules with silicon crystal surface had been studied,[15,16] and Tersoff Si/C potential was used to model the interaction between the C and Si atoms.[15] The researches mentioned earlier using molecular dynamic simulations are mainly focused on the interaction between a particle and one substrate; the particle interacting with two substrates and intruding into a contact space have not been considered.

Recently, we have studied the critical condition for intrusion of a steel ball into sliding contact space by experiment and theoretical analysis.[17] The results showed that there was a critical intrusion angle in the process of intrusion. However, the particle used in our former experiments and analysis was in macroscale; we did not find out the influence factor of particle intrusion process in micro or nano scale. Therefore, now our work emphasises the modelling and simulation of a nanoparticle intrusion process.

In this paper, we used a C60 ball as the smallest ball to simulate the nanoparticle intrusion process. The classical molecular dynamic simulations were conducted with aims to understand the atomic-scale intrusion and friction behaviours of a C60 ball in contact with two flat silicon substrates, and what was more to discuss was whether there was a critical entry angle for a spherical particle in the limitation size.

COMPUTATIONAL MODEL AND METHODOLOGY

A three-dimensional C60 ball–substrates intrusion (here, intrusion means the process wherein the C60 ball moved from the right space, formed by the two substrates, to the left space) system was modelled for the presented computational investigation, as shown in Figure 1.

The material of the lower and upper substrates is silicon (100) with the lattice constant of 0.543 nm. The model consists of a lower substrate of 4145 atoms, an upper substrate of 716 atoms and a C60 ball of 60 atoms. The size selected for lower and upper substrates are $L_{x1} \times L_{y1} \times L_{z1} = 4.344\,\text{nm} \times 10.317\,\text{nm} \times 1.629\,\text{nm}$ and $L_{x2} \times L_{y2} \times L_{z2} = 2.172\,\text{nm} \times 4.887\,\text{nm} \times 1.086\,\text{nm}$, respectively, and the diameter of C60 is 0.71 nm. The upper substrate is inclined, forming an initial entry angle α ranging from 20° to 90°.

DOI: 10.1002/ls

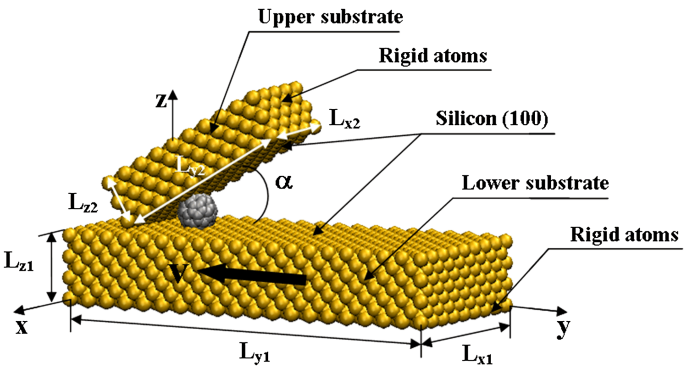

Figure 1. Schematic of Molecular Dynamics simulation model.

The outer one layer of atoms on the bottom side of the lower substrate and the outer one layer of atoms on the right side of the upper substrate are rigid atoms. All the other atoms are thermostat atoms, which are unconstrained as shown in Figure 1.

In the present simulations, the Tersoff potential function, which is the most popular multibody interaction potential (see Zhang and Tanaka[8] and Lin *et al.*[9]), is applied to the interaction among Si atoms and C atoms. If we assume that j and k are the neighbouring atoms of atom i, that the atomic bond lengths of atoms i–j and i–k are r_{ij} and r_{ik}, respectively, and that the angle between bonds i–j and i–k is θ_{ijk}, then the total Tersoff energy E can be expressed as

$$E = \sum_i E_i = \frac{1}{2}\sum_{i \neq j} V_{ij} \tag{1}$$

where V_{ij} is the bond energy, so the summation in the equation is over all the atomic bonds in the control volume. V_{ij} is a function of the repulsive pair potential $\mathrm{f_R}$ and the attractive pair potential $\mathrm{f_A}$, and has the form

$$V_{ij} = \mathrm{f_C}(r_{ij})[\mathrm{f_R}(r_{ij}) + b_{ij}\mathrm{f_A}(r_{ij})] \tag{2}$$

where

$$\mathrm{f_R}(r_{ij}) = A_{ij}\exp(-\lambda_{ij} r_{ij}), \mathrm{f_A}(r_{ij}) = -B_{ij}\exp(-\mu_{ij} r_{ij});$$

$$\mathrm{f_C}(r_{ij}) = \begin{cases} 1, r_{ij} < R_{ij}, \\ \frac{1}{2} + \frac{1}{2}\cos\left[\frac{\pi(r_{ij} - R_{ij})}{(S_{ij} - R_{ij})}\right], R_{ij} < r_{ij} < S_{ij}, \\ 0, r_{ij} > S_{ij}; \end{cases}$$

$$b_{ij} = \chi_{ij}(1 + \beta_i^{n_i}\zeta_{ij}^{n_i})^{-1/2n_i}, \ \zeta_{ij} = \sum_{k \neq i,j} \mathrm{f_C}(r_{ik})g(\theta_{ijk});$$

DOI: 10.1002/ls

$$g(\theta_{ijk}) = 1 + c_i^2/d_i^2 - c_i^2/\left[d_i^2 + (h_i - \cos\theta_{ijk})^2\right];$$

$$\lambda_{ij} = (\lambda_i + \lambda_j)/2,\ \mu_{ij} = (\mu_i + \mu_j)/2,\ A_{ij} = (A_i A_j)^{1/2};$$

$$B_{ij} = (B_i B_j)^{1/2},\ R_{ij} = (R_i R_j)^{1/2},\ S_{ij} = (S_i S_j)^{1/2}.$$

Other parameters such as A, B, R, S, λ, χ and μ, as listed in Table I, are Tersoff potential parameters, depending on the materials. With Equations (1) and (2), the interaction forces between silicon atoms and carbon atoms can be obtained by calculating the gradient of total Tersoff energy E.[18,19]

The classical molecular dynamics with LAMMPS MD code was used in this study. The molecular dynamics simulations were carried out in the NVE ensemble [the system is isolated from changes in moles (N), volume (V) and energy (E) and updates the position and velocity for atoms in the group at each time step]. The simulations were carried out using free rather than periodic boundary conditions. In the simulation model, we maintained the temperature of thermostat atoms at 300 K by rescaling velocities to keep thermostatting procedure.

The lower substrate was then subjected to a constant velocity in the negative y-direction to study the interaction of the C60 ball and the two substrates. To save simulation time, the velocity field was set to 3 nm/ps, and the lower substrate was moved for 3000 steps at a time step of 0.001 ps; this means that the effective displacement of the lower substrate per step was 0.003 nm. Although this velocity may be higher than the speed in tribosystem of laser printer, we think the simulation is helpful to understand the intrusion process with normal speed; in addition, this velocity can be accepted in space stations where the orbital speed is 7.5 km/s.[20]

The positions of all the atoms of the substrates and the C60 ball at every 100 steps were recorded for the visualisation of C60 ball intruding into the sliding contact space. The initial position of the C60 ball was located at the position in the space in where the ball just contacted with the lower substrate in the simulation, i.e. the minimum distance between the atom in C60 and the atom in the upper substrate equaled to the cut-off distance 0.24 nm, which was calculated by $R_{ij}=(R_iR_j)^{1/2}$ (here, R_i=0.18 nm for C, and R_j=0.27 nm for Si).

Table I. Parameters in Tersoff potential for carbon and silicon.[19]

	C	Si
A (eV)	1.3936×10^{3}	1.8308×10^{3}
B (eV)	3.467×10^{2}	4.7118×10^{2}
λ (nm^{-1})	0.34879	0.24799
μ (nm^{-1})	0.22119	0.17322
β	1.5724×10^{-7}	1.1000×10^{-6}
n	7.2751×10^{-1}	7.8734×10^{-1}
c	3.8049×10^{4}	1.0039×10^{5}
d	4.384×10^{0}	1.6217×10^{1}
h	-5.7058×10^{-1}	-5.9825×10^{-1}
R (nm)	0.18	0.27
S (nm)	0.21	0.3
χ_{C-C}=1.0	χ_{Si-Si}=1.0	χ_{C-Si}=0.9776

DOI: 10.1002/ls

RESULTS

The intrusion processes of C60 at different time steps from 400 to 2800 with the initial entry angle α equals to 40° and 80° are shown in Figures 2 and 3, respectively. (Please note that the intrusion processes at the steps from 0 to 400 were not shown here because the change of atoms in the upper substrate is not remarkable in contact region during intrusion in these steps.) For α=40°, C60 first sticks to the lower substrate surface, and after the constant velocity is applied on the lower substrate, C60 will move together with it. When time step equals 400 (Figure 2a), C60 begins to get access to the upper substrate surface. During this time, the force applied on the upper substrate in the *y*-direction and the *z*-direction by C60 is small; thus, the upper substrate does not deform. With the increase of simulation time, C60 continues to move with the lower substrate in the negative *y*-direction, which makes the tip of the upper substrate compressed and the upper substrate starts to deform (Figure 2b). Then, the tip of the upper substrate is lifted, and C60 is just between the two substrates (Figures 2c and 2d). From Figure 2a to Figure 2d we can see that the entry angle formed by the two substrates is becoming smaller, even near 0° as Figures 2c and 2d shows. After C60 passes the sliding contact space, the upper substrate no longer receives the negative *y*-direction and the positive *z*-direction forces applied by C60; meanwhile, the deformation of the upper substrate is recovered (Figures 2e and 2f); even the inverse deformation in the upper substrate appears when the intrusion process was finished (Figure 2g). g). It is clear that during the intrusion process, the adhesion takes place, and some Si atoms of the upper substrate are permanently displaced. In this case, the displaced atoms stick to the lower substrate surface and the C60 ball surface; after that, these atoms move together with them leading to atoms loss of the upper substrate. The number of Si atoms of the upper substrate, which have moved to a distance more than the cut-off distance 0.27 nm from their initial positions (here called sticking atoms), is

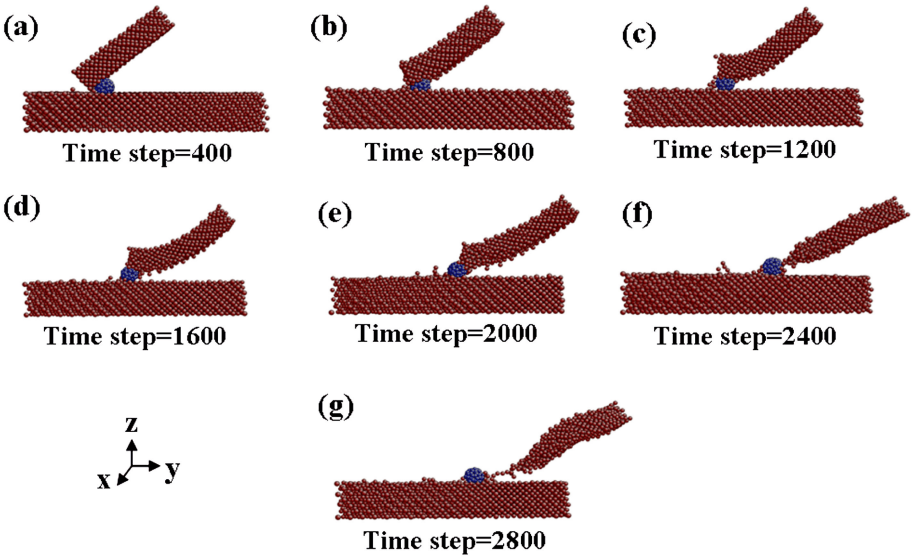

Figure 2. Molecular dynamics simulation results for α=40°.

DOI: 10.1002/ls

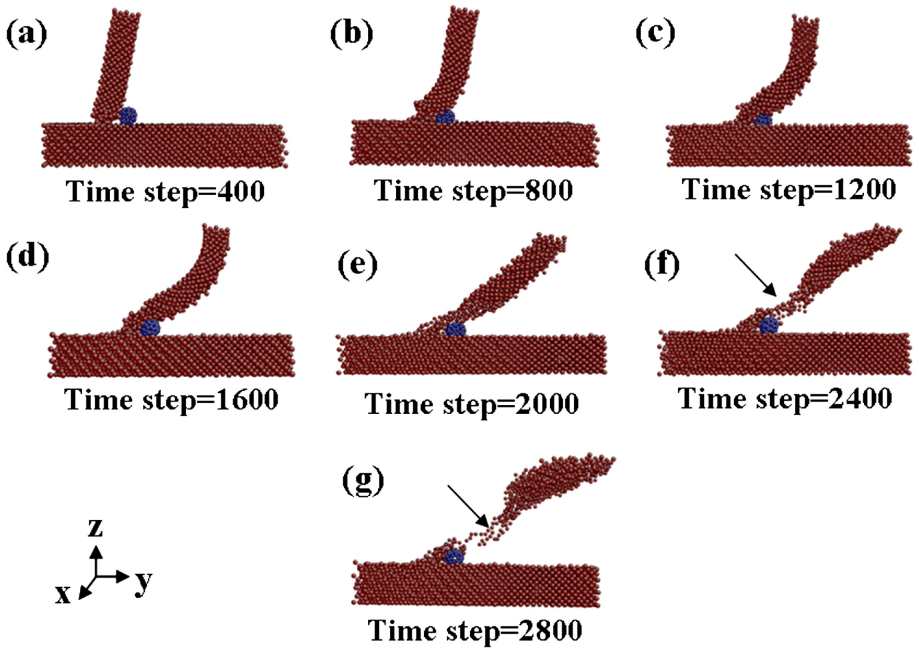

Figure 3. Molecular dynamics simulation results for α=80°.

calculated, and there are 22 sticking atoms on the condition of α=40°. During the whole intrusion process, both sliding and rolling movements of C60 were observed.

The simulation results of C60 intrusion process at the initial entry angle of 80° are not completely the same as the situation of 40°. First, C60 is moving with the lower substrate and approaching the upper substrate (Figure 3a). Later, the upper substrate is compressed by the approaching C60 and begins to deform (Figures 3b–3d). At this time, the upper substrate just experiences a compressing locally without atoms removal. The entry angle is becoming smaller during the intrusion process (Figures 3a–3d), but the minimum value of entry angle is much larger than 0° (in case of Figure 2c, the minimum value of entry angle is near zero). In Figure 3e, it is clearly observed that a large number of atoms near the contact area move from the upper substrate, which indicates that the deformation of the upper substrate is produced because of C60 intrusion. Further intrusion of C60 (see Figures 3f and 3g) leads to adhesions of the tip of the upper substrate to the lower substrate and C60 surfaces; meanwhile, bonds are broken in the Si lattice of the upper substrate, and finally, a number of atoms of the upper substrate (up to the position shown by arrows) were pulled down and stuck to C60 or the lower substrate. C60 cannot completely intrude into the sliding contact space yet be surrounded by the sticking atoms from the upper substrate, which is different from the simulation results as α=40°. This difference shows that the initial entry angle α is an important factor that affects the intrusion process of C60.

In order to find out how the initial entry angle α affects the intrusion process of C60, the simulation is repeated every 2° from 20° to 90°, and Figure 4 only shows the simulation results of every 10° when the time step equals 2000. When the simulation is completed, C60 remains intact, but the upper substrate generates atoms removal (Figures 4a–4h). Atoms removal of upper substrate via adhering in the

DOI: 10.1002/ls

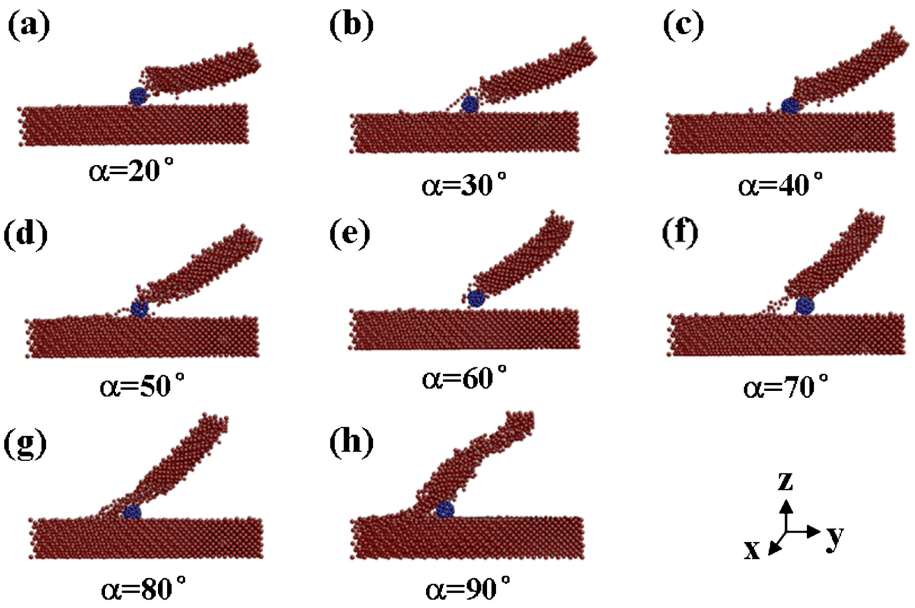

Figure 4. Molecular dynamics simulation results of different initial entry angle.

intrusion process happens because the C–Si interaction is stronger than that of the Si–Si interaction; in addition, Si lattice is brittle and susceptible to more permanent damage during the interactions. In most situations, C60 sticks to the lower substrate after the intrusion process; however, it may stick to the upper substrate surface instead of the lower substrate surface as shown in Figure 4e. When $\alpha \leq 70^\circ$ (Figures 4a–4f), the upper substrate is lifted by C60, and C60 can intrude into the sliding contact space. In addition, less sticking atoms are produced. When $\alpha > 70^\circ$ (Figures 4g and 4h), the upper substrate cannot be lifted, and the C60 is surrounded by the sticking atoms and cannot intrude.

In order to get quantitative evaluation of the intrusion process of C60, we counted the number of sticking atoms of the upper substrate, which moved a distance more than the cut-off distance 0.27 nm from their initial positions at different initial entry angle as shown in Figure 5. The data points in Figure 5 indicate that with increasing initial entry angle, more sticking atoms are produced in the upper substrate, and there exists three different regions with different slopes. When the initial entry angle is less than 70°, the number of sticking atoms is less than 50. Meanwhile, the number of sticking atoms increases slowly with the increasing of initial entry angle. This is because when the initial entry angle is small, the adhesion force between the upper substrate and the C60 ball is small; it just makes some upper substrate atoms stick to the lower substrate and C60. When the initial entry angle is between 70° and 85°, the number of sticking atoms is obviously increased to about 100. In this region, adhesion becomes more serious; meanwhile, more bonds in the upper substrate are broken. When the initial entry angle is greater than 85°, the number grows sharply, and a larger number of atoms of the upper substrate appear to be pulled down and moves together with the lower substrate and C60. Note that the entry angle 85° is a transition point, so it is defined as the critical intrusion entry angle. That implies that when the initial entry angle is less than 85°, the C60 ball can intrude into the sliding contact space,

DOI: 10.1002/ls

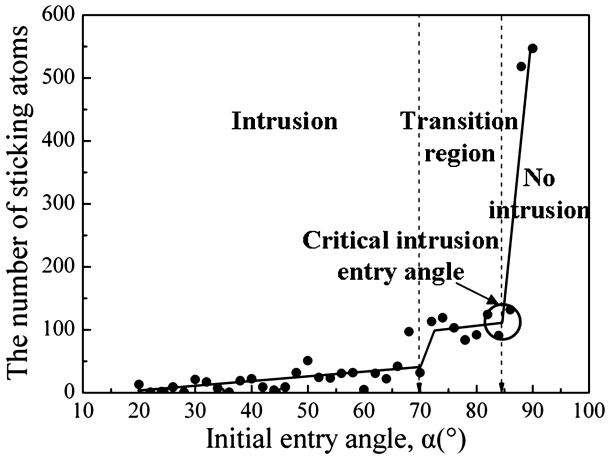

Figure 5. Number of atoms that move a distance more than the cut-off distance at different initial entry angle.

and less sticking atoms are generated; when the initial entry angle is larger than 85°, C60 cannot intrude into the sliding contact space.

DISCUSSION

It should be noted that the simulation results mentioned earlier is mainly about the deformation and atom loss in the upper substrate. This is because the deformation of the lower substrate is small and it does not have obvious effect on the intrusion process of C60; furthermore, in laser printer materials, wear occurs mainly in the upper substrate.[1] However, to gain a deeper insight into the whole intrusion process of C60, the deformation of the lower substrate is shown in Figure 6 when the intrusion process is completed at initial entry angle $\alpha=40°$. Figure 6 shows the top view and the cross section A–A view of the lower substrate, respectively. In Figure 6a, the distance H (about 2 nm) is the horizontal displacement of C60 during the whole intrusion process. Because of the interaction between atoms at C60 and the upper substrate, the lower substrate will suffer a normal force form C60. Hence, the crystal structure of the lower substrate near the contact region is altered, and some atoms of the top atomic layer are displaced. Figure 6b clearly shows that only atoms in the first two layers of the substrate near the contact region are displaced. There is no atom loss (atoms that have moved a distance more than the cut-off distance 0.27 nm from their initial positions) in the lower substrate after the intrusion process; thus, we consider that using atom loss of upper substrate to evaluate the C60 intrusion process is suitable.

On the other hand, we have studied the intrusion process in macroscale, and the results indicate that there is a critical intrusion angle, and when the intrusion angle is less than the critical intrusion angle of about 30°, the ball can intrude without any intrusion normal load; when the intrusion angle is larger than the critical intrusion angle, the intrusion normal load increases as the intrusion angle increases.[17] Our molecular dynamics simulation result in nanoscale is similar as the experimental result in macroscale, there exist a critical intrusion angle 85°, which is larger than that in macroscale case of about

DOI: 10.1002/ls

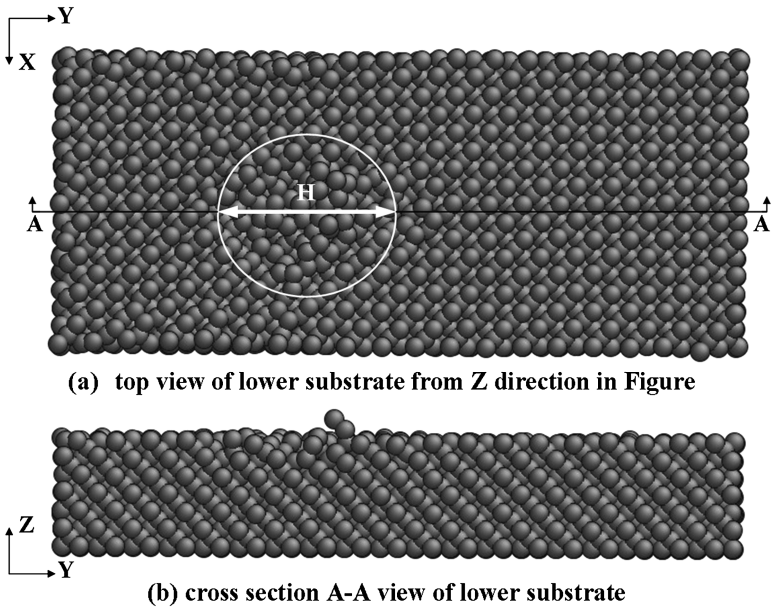

Figure 6. Molecular dynamics simulation results of the lower substrate when α=40°.

30°. Therefore, from the present simulation results, we can draw a conclusion that particle intrusion becomes easier in nanoscale. Hence, in order to clean the spherical particle in nano size in printer, larger entry angle is needed. However, large entry angle will lead to atom loss (wear in macroscale) of upper substrate (blade in printer). Thus, finding out a suitable entry angle that can prevent particle intrusion and produce less atom loss of upper substrate is a problem to be solved in our next work.

Finally, note that the size effects of the ball–substrates intrusion system were not considered. Different sizes fullerenes (such as C70 and C84) or solid spheres will be adopted to investigate the influence of the size of the intrusion ball on the damage profile in our future work.

CONCLUSIONS

Molecular dynamics simulations have been performed to explore C60 intrusion process in a sliding contact space formed by two silicon substrates. With increasing initial entry angle, more sticking atoms are produced in the upper substrate, and the number of sticking atoms is divided into three regions. In the first region, the initial entry angle is below 70°, and the number of sticking atoms is less than 50. In the second region, the initial entry angle is between 70° and 85°, and the number of sticking atoms is obviously increased to about 100. In the last region, the initial entry angle is greater than 85°, and the number grows sharply to about 500. The critical initial entry angle 85° is defined in the process of C60 intrusion. When the initial entry angle is less than the critical initial entry angle, C60 intrudes into the sliding contact space, and less than 100 sticking atoms are produced. Otherwise, a large number of atoms of the upper substrate were pulled down, and C60 cannot intrude.

DOI: 10.1002/ls

ACKNOWLEDGEMENTS

The authors would like to thank the Ricoh Printing System in Japan for their cooperation and the National Nature Science Foundation of China under grant numbers 90923027 and 51050110137 for their support.

REFERENCES

1. Miyasaka T. Tribology in electro-photographic printer. *Tribology in Precision Machines* 2004; **49**:645–650.
2. Murthy PMD, Cetinkaya C. Rolling resistance moment of microspheres on surfaces. *Philosophical Magazine* 2005; **85**(13):1347–1357.
3. Ding W, Howard AJ, Murthy PMD, Cetinkaya C. Rolling resistance moment of microspheres on surfaces: contact measurements. *Philosophical Magazine* 2007; **87**(36):5685–5696.
4. Sitti M, Hashimoto H. Controlled pushing of nanoparticles: modeling and experiments. *IEEE/ASME Transactions on Mechatronics* 2000; **5**:199–211.
5. Shen B, Sun F. Molecular dynamics investigation on the atomic-scale indentation and friction behaviors between diamond tips and copper substrate. *Diamond and Related Materials* 2010; **19**:723–728.
6. Yang J, Komvopoulos K. A molecular dynamics analysis of surface interference and tip shape and size effects on atomic-scale friction., *ASME Transactions, Journal of Tribology* 2005; **127**:513–521.
7. Zhu PZ, Hu YZ, Wang H. Molecular dynamics simulations of atomic-scale friction in diamond–silver sliding system. *Chinese Science Bulletin* 2009; **54**:4555–4559.
8. Zhang LC, Tanaka H. On the mechanics and physics in the nano-indentation of silicon monocrystals. *JSME International Journal* 1999; **42**:546–559.
9. Lin YH, Chen TC, Yang PF, Jian SR, Lai YS. Atomic-level simulations of nanoindentation-induced phase transformation in mono-crystalline silicon. *Applied Surface Science* 2007; **254**:1415–1422.
10. Sanz-Navarro C F, Åstrand P-O, De Chen, Rønning M, van Duin ACT, Mueller JE, Goddard WA III. Molecular dynamics simulations of carbon-supported Ni clusters using the Reax Reactive force field. *The Journal of Physical Chemistry C* 2008; **112**(33):12663–12668.
11. Zhang L, Tanaka H. Atomic scale deformation in silicon monocrystals induced by two-body and three-body contact sliding. *Tribology International* 1998; **31**:425–433.
12. Lee WG, Cho KH, Jang H. Molecular dynamics simulation of rolling friction using nanosize spheres. *Tribology Letters* 2009; **33**:37–43.
13. Rimai DS, Quesnel DJ, Busnaina AA. The adhesion of dry particles in the nanometer to micrometer-size range. *Colloids and Surfaces A: Physicochemical Engineering Aspects* 2000; **165**:3–10.
14. Valentini P, Dumitrica T. Molecular dynamics simulations of nanoparticle–surface collisions in crystalline silicon. *Journal of Nano Research* 2008; **1**:31–39.
15. Beardmore K, Smith R, Webb RP. Energetic fullerene interactions with Si crystal surfaces. *Modelling and Simulation in Materials Science and Engineering* 1994; **2**:313–328.
16. Smith R, Beardmore K, Gras-Marti A. Molecular dynamics simulations of particle–surface interactions. *Vacuum* 1995; **46**:1195–1199.
17. Li F, Diao D, Fan X. The critical condition for intrusion of a steel ball into sliding contact space. *Lubrication Science* 2010; **22**:195–205.
18. Tersoff J. New empirical approach for the structure and energy of covalent systems. *Physical Review B* 1988; **37**: 6991–7000.
19. Tersoff J. Modeling solid-state chemistry: interatomic potential for multicomponent systems. *Physical Review B* 1989; **39**:6991–7000.
20. Brandon A, Krick, W, Gregory S. Space tribometers: design for exposed experiments on orbit. *Tribology Letters* 2011; **41**:303–311.

DOI: 10.1002/ls